Laser ablation resistance and mechanism of Si-Zr alloyed melt infiltrated C/C-SiC composite

Yonggang Tong, Shuxin Bai, Yongle Hu, Xiubing Liang, Yicong Ye, Qing H Qin

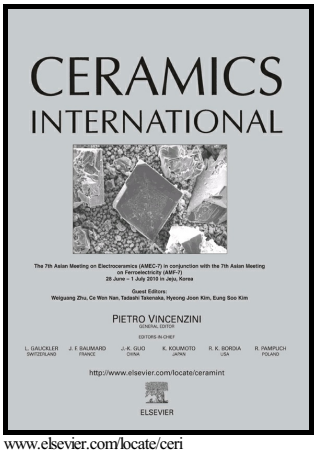

www.elsevier.com/locate/ceri

PII: S0272-8842(17)32599-3
DOI: https://doi.org/10.1016/j.ceramint.2017.11.141
Reference: CERI16796

To appear in: *Ceramics International*

Received date: 27 October 2017
Revised date: 19 November 2017
Accepted date: 19 November 2017

Cite this article as: Yonggang Tong, Shuxin Bai, Yongle Hu, Xiubing Liang, Yicong Ye and Qing H Qin, Laser ablation resistance and mechanism of Si-Zr alloyed melt infiltrated C/C-SiC composite, *Ceramics International,* https://doi.org/10.1016/j.ceramint.2017.11.141

Laser ablation resistance and mechanism of Si-Zr alloyed melt infiltrated C/C-SiC composite

Yonggang Tong [a, 1], Shuxin Bai [b], Yongle Hu [a], Xiubing Liang [c], Yicong Ye [b], Qing H Qin [d]

[a] College of Automobile and Mechanical Engineering, Changsha University of Science and Technology, Changsha, China

[b] College of Aerospace Science and Engineering, National University of Defense Technology, Changsha, China

[c] National Engineering Research Center for Mechanical Product Remanufacturing, Academy of Armored Forces Engineering, Beijing, China

[d] Research School of Engineering, College of Engineering and Computer Science, Australian National University, ACT, Australia

Abstract: Ablation resistance of C/C-SiC composite prepared via Si-Zr alloyed reactive melt infiltration was evaluated using a facile and economical laser ablation method. Linear ablation rates of the composite increased with an increase in laser power densities and decreased with extended ablation time. The C/C-SiC composite prepared via Si-Zr alloyed melt infiltration presented much better ablation resistance compared with the C/SiC composite prepared by polymer infiltration and pyrolysis process. The good ablation resistance of the composite was attributed to the melted ZrC layer formed at the ablation center region. Microstructure and phase composition of different ablated region were investigated by SEM and EDS, and a laser ablation

[1] Corresponding author. Tel.: +86 731 4573145; fax: +86 731 4574791.
E-mail address:tygiaarh419@163.com (YG Tong)

model was finally proposed based on the testing results and microstructure characterization. Laser ablation of the composite experienced three distinct periods. At the very beginning, the laser ablation was dominated by the oxidation process. Then for the second period, the laser ablation was dominated by the evaporation, decomposition and sublimation process. With the further ablation of the composite, chemical stable ZrC was formed on the ablated surface and the laser ablation was synergistically controlled by the scouring away of ZrC melts and evaporation, decomposition and sublimation process.

Keywords: C/C-SiC composite; laser ablation; microstructure; ablation mechanism; reactive melt infiltration

1. Introduction

Carbon fiber reinforced C, SiC binary matrix composite (C/C-SiC) is an attractive candidate for highly demanding engineering applications such as heat shields, structural components for re-entry space vehicles, high performance brake discs and high temperature heat exchanger tubes due to its unique combination of low density, high hardness, excellent oxidation resistance, high strength, thermal shock resistance and damage tolerance [1-3]. However, the maximum working temperature of C/C-SiC composite is limited at about 1650^{o}C due to the active oxidation of silica layer in oxygen-containing atmosphere and the stress-oxidation coupling effect that follows [4, 5]. Introduction of ultra-high temperature ceramics (UHTCs) such as refractory carbides, borides and silicides into the matrix of the composite has been thought to be a potentially effective approach to improve the ablation and oxidation resistance of

the C/C-SiC composites at higher temperatures [6, 7]. In the family of UHTCs, zirconium-bearing UHTCs have received a considerable attention due to their ultra-high melting temperatures, relatively low density and ablation-resistant oxide scale formed in the ablation process [8, 9]. Great efforts have been made to introduce zirconium-bearing UHTCs into the C/C-SiC composites and several modified C/C-SiC composites have been developed. Wang et al [10] studied the effects of inter-phases on the mechanical properties and microstructure of the C/SiC-ZrC composites fabricated by firstly mold-pressing and then polymer infiltration and finally pyrolysis process. Padmavathi et al [11] prepared a carbon-fiber reinforced (SiC+ZrC) mini-composite by soft-solution approach and evaluated the effect of ZrC content on the mechanical strength of the composite. Hu et al [12] prepared a C/SiC-ZrB_2 composite by slurry and precursor infiltration and pyrolysis method and investigated the bending strength of the composite at room and high temperature. In our previous work [13-15], a quick and low cost alloyed reactive melt infiltration process has been developed to introduce the zirconium-bearing UHTCs into the C/C-SiC composite. The composite showed high mechanical strength and good oxidation resistance. Wang et al [16] also prepared the modified C/C-SiC composite by this low cost and quick reactive melt infiltration process and studied the microstructure and properties of the composite.

Ablation resistance is one of the most important properties evaluating the usability of high temperature materials [17]. It is of great significance to validate the ablation properties of zirconium-bearing UHTCs modified C/C-SiC composite before its

practical application in the ablation environment. Recently, the laser beam has been used to evaluate the ablation-resistance of UHTCs coatings and UHTCs composites [18-20], indicating that laser ablation is a facile, reliable and low cost method to evaluate ablation resistance of materials. Moreover, the evaluation of material's ablation resistance by laser beam provides us more knowledge about the usability of materials and developing protection against laser irradiation. However, few reports are currently available on the laser ablation evaluation of zirconium-bearing UHTCs modified C/C-SiC composite. The ablation mechanism under the condition of rapid thermal impact like laser beam is still unclear until now.

In our previous work [13, 14], zirconium-bearing UHTCs modified C/C-SiC composites have been produced by alloyed melt infiltration using silicon based Si-Zr alloys. The aim of the present work is to evaluate the ablation resistance of the Si-Zr alloyed melt infiltrated C/C-SiC composite using a pulsed laser beam. The microstructure and ablation rate of the composite was firstly characterized. A laser ablation mechanism was finally proposed on the basis of the experiment investigation.

2. Experimental

2.1 Material preparation

Carbon fiber needled felts were used as reinforcements. The carbon fibers were PAN-based (T300, Toray, Japan). The needled felts were prepared by a three-dimensional needling technique, starting with repeatedly overlapping the layers of 0°non-woven fiber cloth, short-cut-fiber web, and 90°non-woven fiber cloth with needle-punching step by step. Pyrolytic carbon was deposited on the carbon fibers to

prepare a porous C/C preform by chemical vapor infiltration (CVI) process. The porous C/C preform was cut, polished, ultrasonically cleaned with ethanol and dried at 100℃ for 4 h. C/C-SiC composite was then prepared by infiltrating the porous C/C preform with a Si-Zr10 alloyed melts (Si: 90 at.%, Zr: 10 at.%). The details of the reactive melt infiltration process have been previously reported in Ref. [13]. The C/C-SiC composite prepared by Si-Zr alloyed reactive melt infiltration present work was labeled as Si-Zr ARMI-C/C-SiC composite.

2.2 Ablation testing

The ablation resistance of the Si-Zr ARMI-C/C-SiC composite was tested by a pulsed laser beam in the air. The laser ablation equipment is a Nd: YAG pulsed laser (wave length 1.064 μm) with the following parameters: frequency 20 Hz, pulse width 1 ms, laser spot diameter about 1.5 mm. The average laser power densities varied from 150W/cm^2 to 1500W/cm^2. During the ablation testing, the C/C-SiC composite was placed in a test chamber and then vertically irradiated by the pulsed laser. The ablation depth of the composite was given by the thickness changes before and after the ablation test. The linear ablation rate of the composite was calculated by the eroded depth at the ablation center dividing the ablation time. As a comparison, the ablation resistance of the C/SiC composite prepared by polymer infiltration and pyrolysis process (labeled as PIP-C/SiC composite) was also tested by the laser beam under the same condition. Three-dimensional braided carbon fiber preform was used as the reinforcement for the PIP-C/SiC composite. The density of the as-produced PIP-C/SiC composite is 1.91g/cm^3 and the open porosity is about 11.3%.

2.3 Characterization

The morphologies of the composites were observed by a Hitachi-S4800 scanning electron microscope (SEM). The chemical composition was examined by energy dispersive spectroscopy (EDS). The phases were identified by X-ray diffraction (XRD, Rigaku D/Max 2550VB-) using a Ni-filtered Cu Kα radiation at a scanning rate of 5°/min and scanning from 15° to 80° of 2θ.

3. Results and discussion

3.1 Microstructure and composition of the C/C-SiC composite

Fig.1 shows the XRD patterns of the C/C-SiC composite prepared by Si-Zr alloyed reactive melt infiltration. The phases in the composite are SiC, C and $ZrSi_2$. No detectable residual infiltrated alloy phase peaks was found. Fig.2 shows the typical cross-section microstructure of the composite. As can be seen, the Si-Zr alloyed melt was infiltrated into both the large pores among adjacent carbon fiber bundles and some small pores among carbon fibers in the porous C/C preform. A dense C-SiC-$ZrSi_2$ matrix with a SiC layer around pyrolytic carbon inside the pores of C/C preform and $ZrSi_2$ in the middle area of pores surrounded by the SiC layer is formed in the Si-Zr alloyed melt infiltrated C/C-SiC composite.

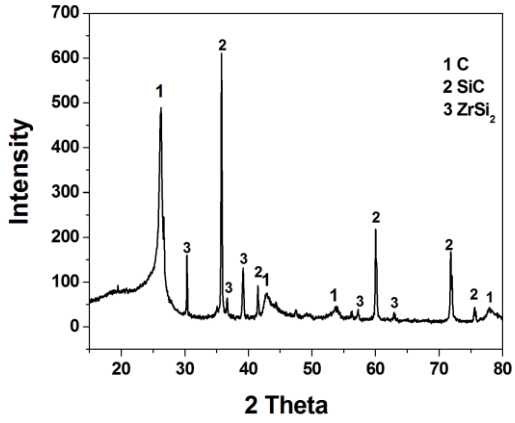

Fig.1 XRD patterns of the Si-Zr ARMI-C/C-SiC composite.

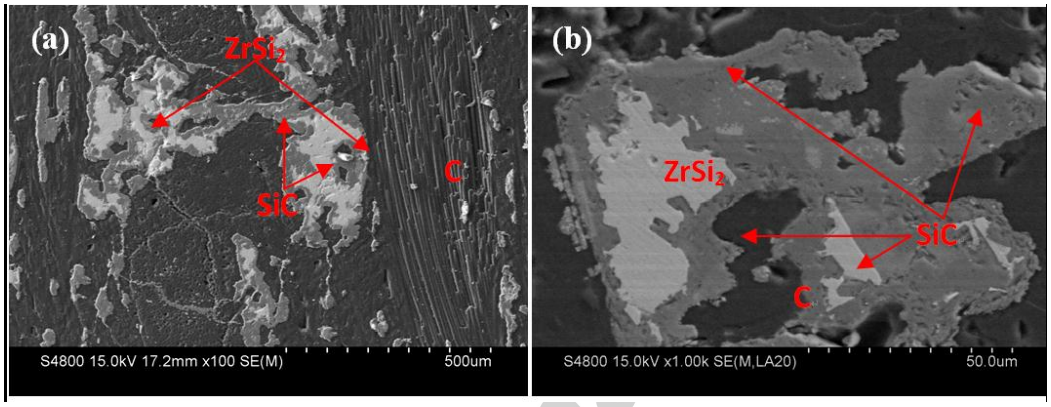

Fig.2 Typical cross-section microstructure of the Si-Zr ARMI-C/C-SiC composite.

(a) × 100 (b) ×1000

3.2 Ablation-resistant properties

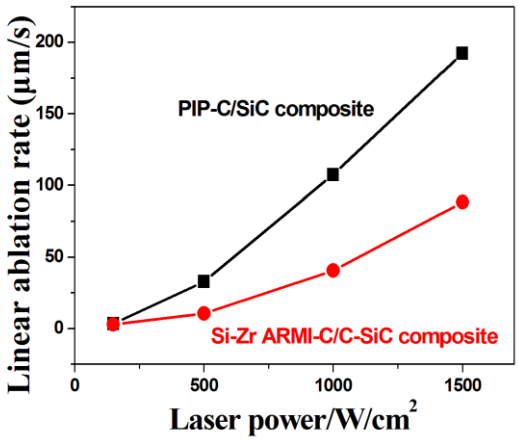

Fig.3 Linear ablation rates of the Si-Zr ARMI-C/C-SiC composite and PIP-C/SiC composite versus the laser power densities.

Fig. 3 shows the linear ablation rates of the Si-Zr ARMI-C/C-SiC composite and the PIP-C/SiC composite versus the laser power densities. As can be seen, the linear ablation rates of both the composites increase with increasing laser power densities. The linear ablation rate of the Si-Zr ARMI-C/C-SiC composite is much smaller than that of the PIP-C/SiC composite. With increasing laser power densities, the difference in linear ablation rates between the two composites increases, indicating that the ablation resistance of the Si-Zr ARMI-C/C-SiC composite is greatly improved at higher temperatures. During the ablation process, the laser energy is absorbed by the composite with an absorption coefficient, a heat conduction width and a heat penetration depth [21]. The conduction laser energy along the heat penetration depth and conduction width decreases progressively from its input value, which in turn can affect the corresponding temperature distribution. The higher the laser power density generally corresponds to the greater the heat penetration depth. Exposed in the laser beam with low power densities, the temperature of the composite during ablation is low. Thus, the linear ablation rates of both the composites are quite low and just show a very small difference (see Fig.3). When the composites are ablated by the laser beam with higher power densities, the temperature during ablation becomes higher and meanwhile, the difference of linear ablation rates between the two composites is enlarged. Due to the zirconium based phase introduced into the C/C-SiC composite, the ablation resistance of the composite at the high temperatures is greatly improved and presents much smaller linear ablation rates than that of the PIP-C/SiC composite. Linear ablation rates of the Si-Zr ARMI-C/C-SiC composites tested at the laser power

densities of 1000 and 1500 W/cm^2 are 40.7 and 88.3 μm/s, respectively, much smaller than that of the PIP-C/SiC composite, 107.6 and 192.4μm/s.

In order to evaluate the ablation resistance of the Si-Zr ARMI-C/C-SiC composite at a constant temperature, here, the Si-Zr ARMI-C/C-SiC composite and the PIP C/SiC composite were tested with a constant power densities of 1000W/cm^2 for different time intervals. The linear ablation rates of the two composites ablated for different time intervals are shown in Fig.4. It is indicated that the linear ablation rates of both the composites decrease with the extension of ablated time. The difference of the linear ablation rates between two composites keeps approximately constant for different time intervals, which further demonstrates the much better ablation resistance of the Si-Zr ARMI-C/C-SiC composite. Linear ablation rates of the Si-Zr ARMI-C/C-SiC composite is approximately half of that of the PIP-C/SiC composite for different ablation time intervals.

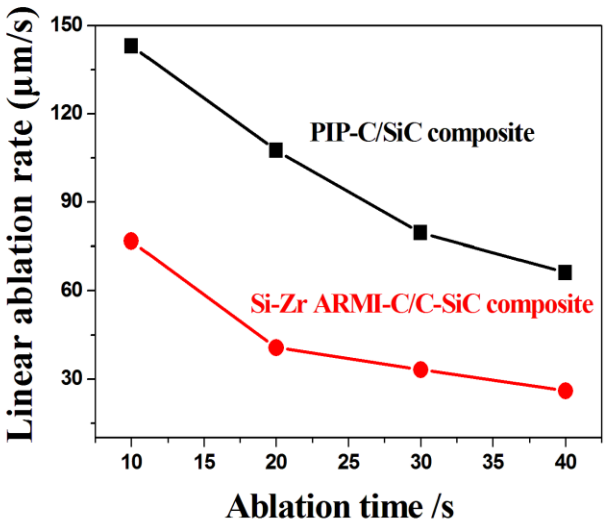

Fig.4 Linear ablation rates of the Si-Zr ARMI-C/C-SiC composite and PIP-C/SiC composite versus the ablation time.

3.3 Ablation morphology

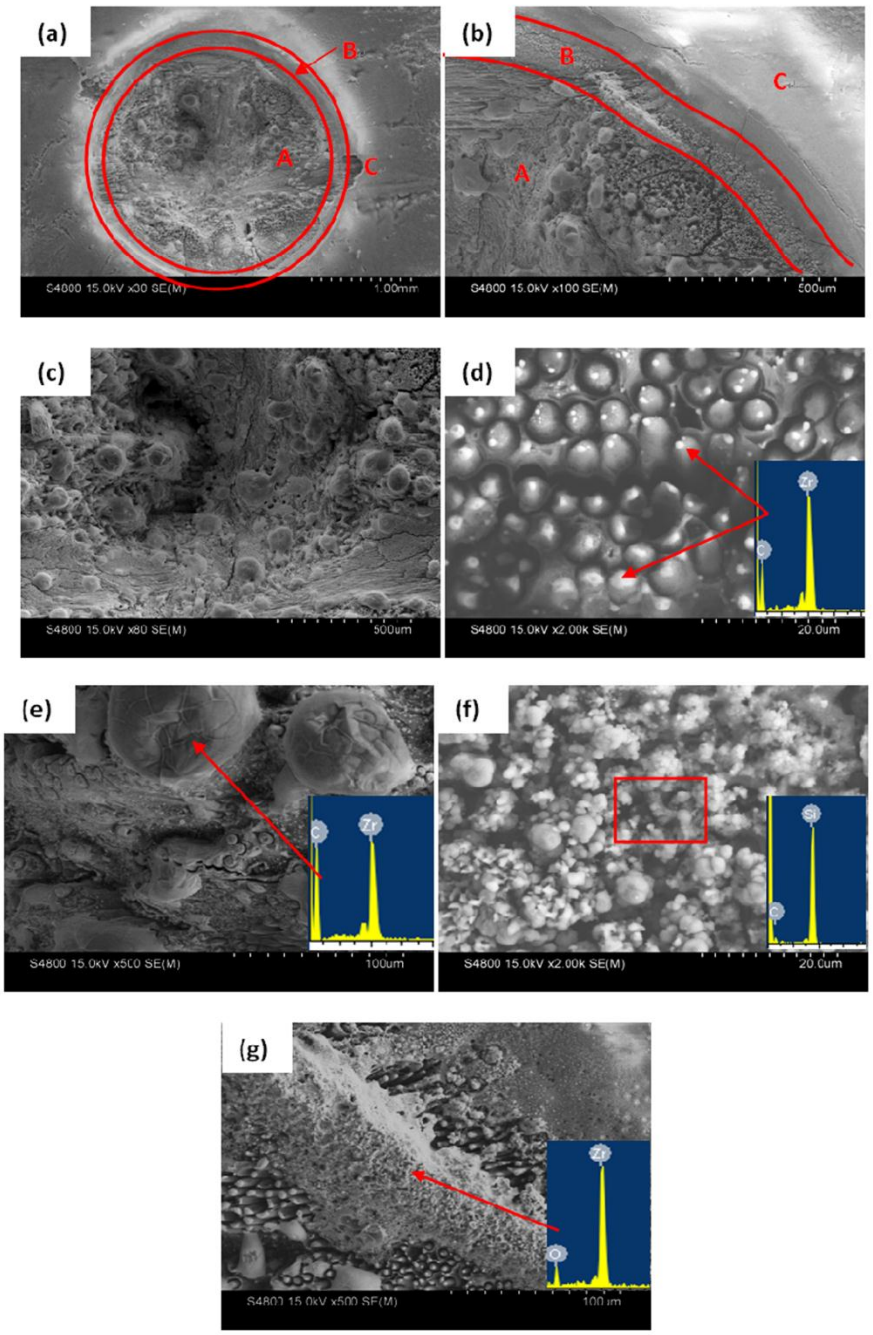

Fig.5 Surface morphologies of the Si-Zr ARMI-C/C-SiC composite ablated at 1000 W/cm^2 for 10s (a) and (b) three ablated regions on the ablated surface; (c) macro morphologies of the ablation center; (d) some small droplet on the ablated carbon fibers and pyrolytic carbon; (e) large magnification morphologies of the ZrC layer; (f) large magnification morphologies of the particles in transition zone; (g) ZrO_2 particles in some partial areas of transition zone.

Fig. 5 shows the ablated surface morphologies of the Si-Zr ARMI-C/C-SiC composite at 1000W/cm^2 for 10s. Three distinct regions can be found on the ablated surface from the center to the boundary: region A ablation center with a deep pit, region B transitional zone with a lot of particles and region C ablation edge covered by a white glassy layer (Fig. 5(a) and (b)). The detailed SEM observations of region A (Fig.5(c and e)) show that a thin discontinuous melted layer, which is characterized as ZrC by EDS, covers the central region with the ablated carbon fibers and pyrolytic carbon underlying it. Some small droplets and grains (Fig.5 (d)), which are also ZrC determined by EDS, can be observed on the ablated carbon fibers and pyrolytic carbon. ZrC, known as a member of ultra high temperature ceramic family, has an extremely high melting point, high strength, high hardness and excellent high temperature ablation resistance [22], which can well protect the composite from the subsequent ablation. The melted ZrC layer exhibits bubbles, which are adherent to the ablated surface and their formation will be discussed later. Compared with the Si-Zr ARMI-C/C-SiC composite, the ablated center of the PIP-C/SiC composite shows a deep pit without any protecting layer (see Fig.6). That is the reason why the Si-Zr ARMI-C/C-SiC composite presents much better ablation resistance than the PIP-C/SiC composite. In region B transitional zone, there are lots of spherical particles (Fig.5 (f)), which are SiC phase with a composition of silicon and carbon owning the atom proportion of 54.47:45.53 determined by EDS. In some partial areas of region B, some ZrO_2 particles were also found by EDS (Fig.5 (g)). The white layer in the region C ablation edge is SiO_2 determined by EDS. The edge of this region

adjacent to region B shows a small bump, which may be piled up by the ablated product from the ablation center.

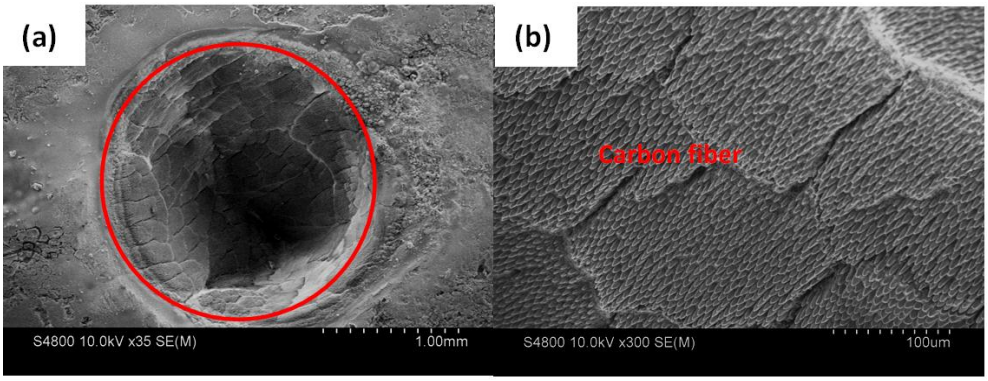

Fig.6 Surface morphologies of the PIP-C/SiC composite ablated at 1000 W/cm^2 for 10s (a) the ablated deep pit on the ablated surface; (c) large magnification morphologies of the ablation center.

The above three ablated regions can be more clearly seen on the surface morphologies of the Si-Zr ARMI-C/C-SiC composite ablated at 1000 W/cm^2 for 30s (Fig.7). As the ablation time increases, more severely ablation with a deeper pit is observed. The ablation center shows the similar discontinuous ZrC melted layer with the composite ablated at 1000W/cm^2 for 10s. Nevertheless, much more ZrO_2 (determined by EDS) were observed in region B transitional zone. ZrO_2 appears like the melted ZrC bubbles adhered to the ablated surface, which is thought to be formed by the in situ oxidation of the ZrC bubbles. Region C ablation edge as shown in Fig.7(c) is covered by a white glassy SiO_2 layer without any difference from the composite ablated at 1000W/cm^2 for 10s.

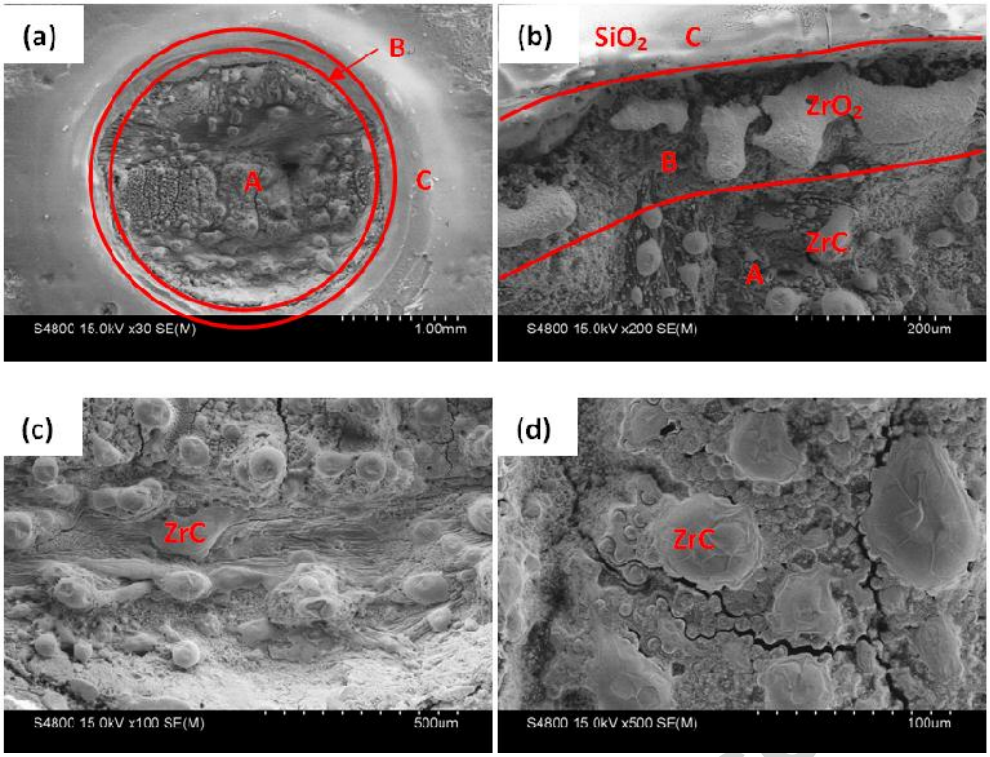

Fig.7 Surface morphologies of the Si-Zr ARMI-C/C-SiC composite ablated at 1000W/cm^2 for 30s (a) and (b) three ablated regions on the ablated surface; (c) macro morphologies of the ablation center; (d) large magnification morphologies of the ZrC layer.

3.4 Ablation mechanism

Ablation is an erosive phenomenon with a removal of material by the combination of thermo-mechanical, thermo-chemical and thermo-physical factors [23]. The microstructure characterization of the different ablation regions as shown above may offer some information in understanding the ablation mechanism for the Si-Zr ARMI-C/C-SiC composite.

During the ablation testing, the center region of the ablated surface was instantly heated to a very high temperature, which was estimated to be higher than 3500℃ [24]. Undoubtedly, the evaporation, decomposition and sublimation of the phases in the composite exposed to such extremely high temperature take place, and finally form a

hot mixture of gases and vapors. SiC with relatively low thermally stable temperature of 2700^{o}C decomposes and sublimates. Carbon fibers and pyrolytic carbon get to their sublimation temperature to form a carbon vapor. $ZrSi_2$ in the composite melts and evaporates, and probably decompose at such a high temperature. The above chemical and physical changes within the central region of the ablated surface are shown as follows:

$$SiC(s)\rightarrow Si(g)+C(g) \quad (1)$$

$$C(s)\rightarrow C(g) \quad (2)$$

$$ZrSi_2(s)\rightarrow ZrSi_2(l) \rightarrow ZrSi_2(g) \quad (3)$$

$$ZrSi_2(s) \rightarrow Zr(g)+Si(g) \quad (4)$$

Additionally, the ablation testing was performed in the air and the phases in the composite can be oxidized to form a mixed gas of CO, CO_2, SiO, SiO_2 and ZrO_2 due to the reaction with oxygen according to Eq. (5-10). Note that the mixed gas will result in a positive pressure atmosphere on the ablation surface. The oxygen close to the ablation surface can be instantly exhausted and the oxygen in the outer atmosphere can hardly diffuse into the atmosphere close to the ablation surface due to the positive pressure kept by the mixed gasses and vapors produced according to Eq. (1-4). Given that the oxidation of the composite in the center region is consider to occur at the very beginning stage and it, therefore, will not be considered in the subsequent ablation process, which would not affect the reasonability of our analysis.

$$SiC(s)+O_2(g)\rightarrow SiO(g)+CO(g) \quad (5)$$

$$SiC(s)+O_2(g)\rightarrow SiO_2(g)+CO(g) \quad (6)$$

$$C(s)+O_2(g)\rightarrow CO(g) \quad (7)$$

$$C(s)+O_2(g)\rightarrow CO_2(g) \quad (8)$$

$$ZrSi_2(s)+O_2(g)\rightarrow SiO_2(g)+ZrO_2(l) \quad (9)$$

$$ZrO_2(l)\rightarrow ZrO_2(g) \quad (10)$$

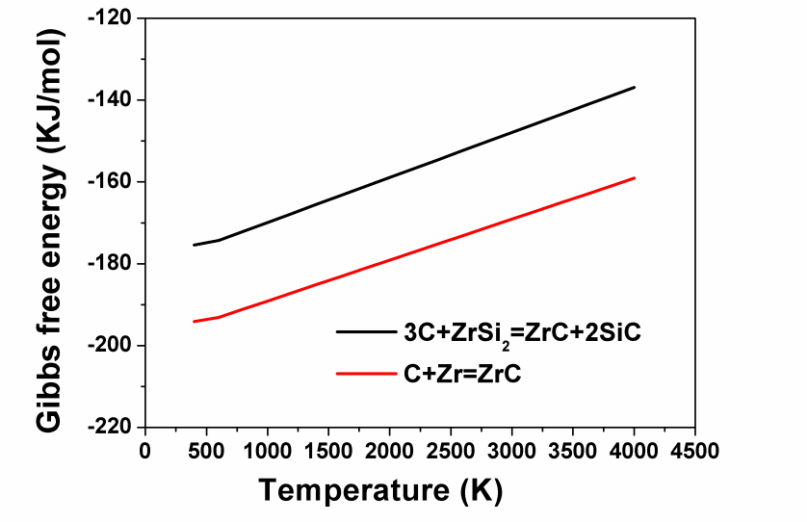

Fig.8 Changes in Gibbs free energy as a function of temperature.

According to Eq. (1-4), the mixed gases and vapors containing C(g), $ZrSi_2$(g), Si(g) and Zr(g) are formed. Most of them are pulled out of the ablated pit and the composite suffers severely ablation. However, Zr(g) and $ZrSi_2$(g) can react with C(g), carbon fibers and pyrolytic carbon in the composite to form a ZrC phase according to Eq. (11-13). Additionally, $ZrSi_2$ phase in the composite may also react with C(g) and pyrolytic carbon in the composite to form a ZrC phase according to Eq. (14-15). Gibbs' free energy changes of reaction between Zr, $ZrSi_2$ and carbon are shown in Fig.8. The negative values of the Gibbs' free energy changes indicate that reactions (11-15) are strongly favored thermodynamically. The ZrC layer observed on the ablation center can further demonstrate the reaction formation of ZrC (Fig.5 and 7).

ZrC with a melting point of 3500^{o}C is chemically stable in the ablated center. It melts at the high temperature of the ablation center and flows onto the composite surface, which is believed to protect the composite from severe ablation. Reduction of the composite's linear ablation rates with extension of ablation time can also demonstrate the protection of ZrC layer for the composite. Nevertheless, the ZrC layer as shown in Fig.5 and 7 is discontinuous. Therefore, Most of the composite surface is still exposed in the laser beam and the composite is ablated with a reduced ablation rate. Because ZrC is in a liquid state, it is blown up by the gases or vapors produced according to Eq. (1-4) and presents like bubbles adhered to the ablated surface (Fig.5 and 7).

$$C(g)+Zr(g) \rightarrow ZrC(l) \quad (11)$$

$$ZrSi_2(g)+C(g) \rightarrow SiC(g)+ZrC(l) \quad (12)$$

$$ZrSi_2(g)+C(s) \rightarrow SiC(g)+ZrC(l) \quad (13)$$

$$ZrSi_2(s)+C(s) \rightarrow SiC(s)+ZrC(s) \quad (14)$$

$$ZrSi_2(s)+C(g) \rightarrow SiC(g)+ZrC(l) \quad (15)$$

At the region B transitional zone of the ablation surface, the conducted heat and the corresponding heat penetration depth are much lower than that at the ablation center. It is not high enough to induce the decomposition, vaporization and sublimation of the phases in the composite. The mixed gases of C(g), $ZrSi_2$(g), Si(g) and Zr(g) escaping from the ablation center are cooled down, and the SiC grains re-nucleate and grow to spherical particles (see Fig. 5(f)). Moreover, ZrC may also be formed according to Eq. (11) and $ZrSi_2$ may deposit on some partial areas of region B due to the cooling down of the mixed gases escaped. ZrO_2 particles in some partial areas of region B (Fig.5

and 7) may be resulted from the oxidation of $ZrSi_2$ or ZrC. Though the temperature at the transitional zone is lower than that of the ablation center, it is believed to be high enough to enable the volatilization of SiO_2 (the boiling point 2230℃ [25]). Thus, no SiO_2 was found at the transitional zone. At region C ablation edge, the heat is only conducted from the ablation center and the temperature is the lowest. The composite is merely suffered oxidized and the generated SiO_2 resulted from the oxidation is not volatilized. Therefore, the as-irradiated region is covered by a white glassy SiO_2 layer (Fig. 5(b)).

The laser ablation behavior of materials strongly depends on their structures and properties [26]. In order to understand the laser ablation processes of the Si-Zr ARMI-C/C-SiC composite, an ablation model based on the previous characterization results and discussion is proposed as illustrated in Fig. 9. The procedure is described as follows.

At the very beginning of the ablation, carbon, SiC and $ZrSi_2$ phases in the composite are oxidized due to the reaction with oxygen in the atmosphere according to Eq. (5-10), which forms a mixed gas of CO, CO_2, SiO, SiO_2 and ZrO_2. The mixed gas leading to a positive pressure atmosphere on the ablation surface is blown out of the ablation center region. The laser ablation for this first stage is dominated by the oxidation process of the phases in the C/C-SiC composite (Fig.9 (a)).

The oxygen in the atmosphere over the ablation surface is believed to be instantly exhausted by the oxidation of the composite because oxygen is merely 21vol% in the outside atmosphere and the oxygen in the outside atmosphere can hardly diffuse into

the atmosphere over the ablation surface due to the positive pressure kept by the mixed gasses and vapors produced according to Eq. (1-4). At the very high temperature heated by the laser beam, the phases in the composite reach their evaporation, decomposition and sublimation temperatures to form a hot mixture of gases and vapors and then escape from the surface of ablated center. The laser ablation for this second stage is dominated by the evaporation, decomposition and sublimation process (Fig.9 (b)).

With the further ablation of the composite, chemical stable ZrC is formed by the reaction according to Eq. (11-15). ZrC at the high temperature in the ablation center is of a liquid state, and flows onto the composite surface, which protect the composite from severely further ablation. With extension of ablation time, more ZrC is formed and the composite presents a decreasing linear ablation rates. Because ZrC in the ablated center is of a liquid state, some may be scoured away by the mixed gases or the laser beam in the subsequent ablation process. In this stage, the laser ablation is synergistically controlled by scouring away of ZrC melt, together with evaporation, decomposition and sublimation process (Fig.9 (c)).

The laser ablation of the Si-Zr ARMI-C/C-SiC composite experiences the above three periods. The formation of the liquid ZrC melt effectively protects the composite from the subsequent severe ablation. Thus, the Si-Zr ARMI-C/C-SiC composite presents much better ablation resistance than the PIP-C/SiC.

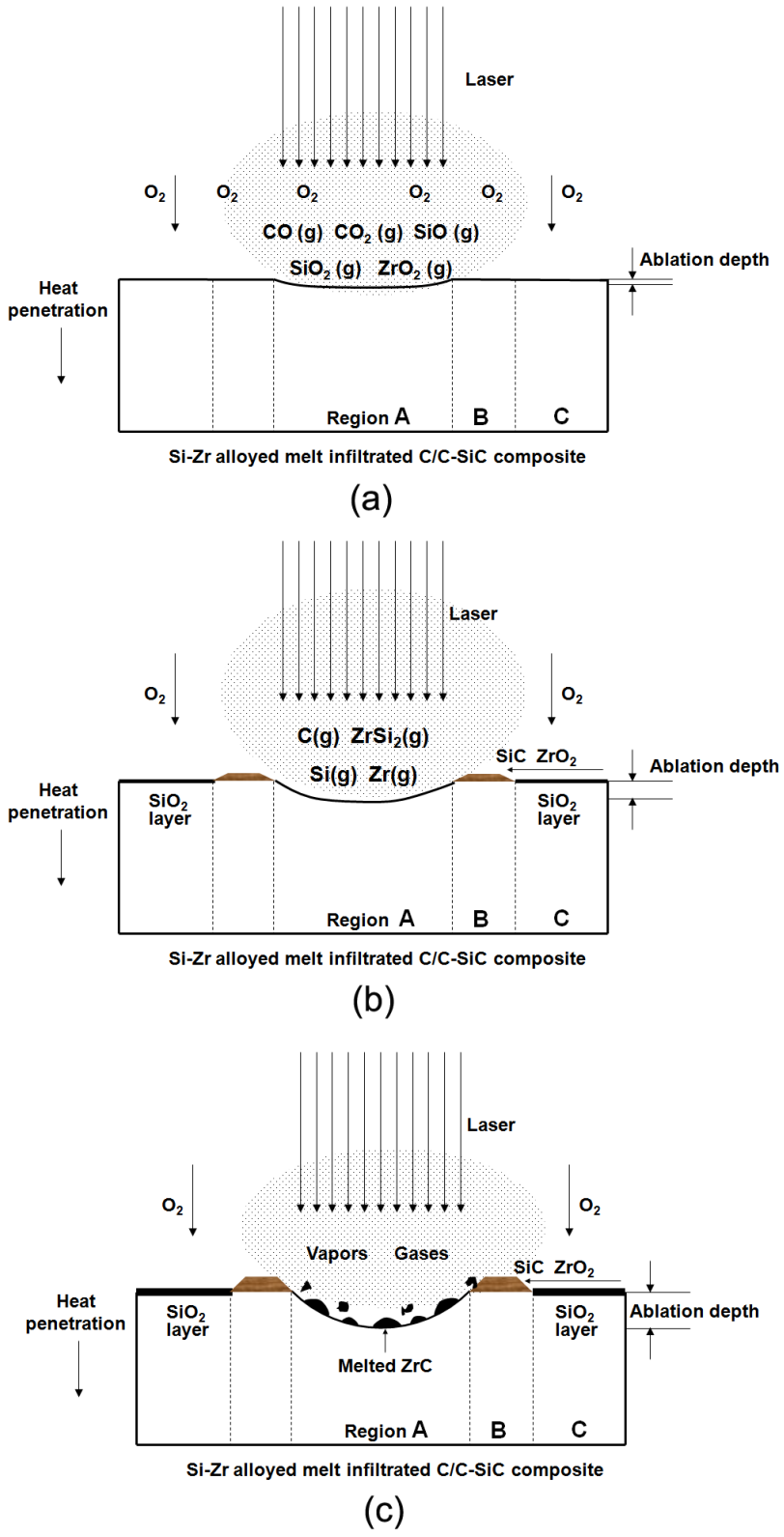

Fig.9 Laser ablation model for the Si-Zr ARMI-C/C-SiC composite (a) first stage dominated by the oxidation process; (b) second stage dominated by evaporation, decomposition and sublimation process; (c) third stage synergistically controlled by the scouring away of ZrC melt and evaporation, decomposition and sublimation process.

4. Conclusion

Laser ablation was demonstrated to be a facile method to investigate the ablation resistance of the Si-Zr ARMI-C/C-SiC composite. The linear ablation rates of the composite increased with increasing laser power densities and decreased with the extended ablation time intervals. Melted ZrC layer was formed at the ablation center, effectively protecting the composite from severe ablation damage. Laser ablation of the composite was thought to experience three distinct periods. At the very beginning, the composite merely suffered the oxidation of its phases. Then for the second period, the laser ablation damage became dominated by the evaporation, decomposition and sublimation process. With the further ablation of the composite, chemical stable and ablation-resistant ZrC was formed on the ablated surface and the laser ablation was controlled by the scouring away of ZrC melts together with the evaporation, decomposition and sublimation process.

Acknowledgments

This work is supported by National Natural Science Foundation of China (51641502).

References

[1] Y.Y. Cui, A.J. Li, B. Li, X. Ma, R.C. Bai, W.G. Zhang, et al. Microstructure and ablation mechanism of C/C–SiC composites, J. Eur. Ceram. Soc. 34(2014)171-177.

[2] W. Krenkel, Application of fiber reinforced C/C-SiC ceramic, Ceram. Forum. Int. 80(8)(2003)31-38.

[3] Y. Li，P. Xiao，H. Luo，R. Almeida，Z. Li, W. Zhou, et al. Fatigue behavior and

residual strength evolution of 2.5D C/C-SiC composites, J. Eur. Ceram. Soc. 36 (16) (2016) 3977-3985.

[4] Q.G. Li, S.M. Dong, Z. Wang, P. He, H.J. Zhou, J.S. Yang, et al. Fabrication and Properties of 3-D C/SiC–ZrC Composites, Using ZrC Precursor and Polycarbosilane, J. Am. Ceram. Soc. 95 (4) (2012) 1216-1219.

[5] Q.M. Liu, L.T. Zhang, J. Liu, X.G. Luan, L.F. Cheng, Y.G. Wang, The oxidation behavior of SiC-ZrC-SiC-coated C/SiC mini composites at ultrahigh temperatures, J. Am. Ceram. Soc. 93 (12) (2010) 3990-3992.

[6] S.F. Tang, J.Y. Deng, S.J. Wang, W.C. Liu, K. Yang, Ablation behaviors of ultra-high temperature ceramic composites. Mater. Sci. Eng. A 465(2007)1-7.

[7] L. Li, Y. Wang, L. Cheng, L. Zhang, Preparation and properties of 2D C/SiC–ZrB2–TaC composites, Ceram. Int. 37 (2011) 891-896.

[8] H.B. Li, L.T. Zhang, L.F. Cheng, Y.G. Wang, Fabrication of 2D C/ZrC–SiC composite and its structural evolution under high temperature treatment up to 1800 ^{o}C, Ceram. Int. 35(2009)2831-2836.

[9] S.A. Chen, C.R. Zhang, Y.D. Zhang, D.Zhao, H.F. Hu, Z.B. Zhang, Mechanism of ablation of 3D C/ZrC-SiC composite under an oxyacetylene flame, Corros. Sci. 68 (2013) 168-175.

[10] Z. Wang, S.M. Dong, Y.S. Ding, X.Y. Zhang, H.J. Zhou, J.S. Yang, et al. Mechanical properties and microstructures of C/SiC–ZrC composites using T700SC carbon fibers as reinforcements, Ceram. Int. 37(2011)695-700.

[11] N. Padmavathi, S. Kumari, V.V. Bhanu Prasad, J. Subrahmanyama, K.K. Ray,

Processing of carbon-fiber reinforced (SiC+ZrC) mini-composites by soft-solution approach and their characterization, Ceram. Int. 35(2009)3447-3454.

[12] H.F. Hu, Q.K. Wang, Z.H. Chen, C.R. Zhang, Y.D. Zhang, J. Wang, Preparation and characterization of C/SiC–ZrB2composites by precursor infiltration and pyrolysis process, Ceram. Int. 36 (2010) 1011-1016.

[13] Y.G. Tong, S.X. Bai, H. Zhang, K. Chen, C/C-SiC composite prepared by Si-10Zr alloyed melt infiltration, Ceram. Int. 38 (4) (2012) 3301-3307.

[14] Y.G. Tong, S.X. Bai, H. Zhang, Y.C. Ye, Effect of C/C preform density on microstructure and mechanical properties of C/C-SiC composites prepared by alloyed reactive melt infiltration, Mater. Sci. Technol. 28 (12) (2012) 1505-1512.

[15] Y.G. Tong, Y.C. Ye, S.X. Bai, H. Zhang, Effects of zirconium addition on microstructure and ablation resistance of carbon fibre reinforced carbon and SiC ceramic matrix composite prepared by reactive melt infiltration, Adv. Appl. Ceram. 113(5)(2014)307-310.

[16] Y.G. Wang, X.J. Zhu, L.T. Zhang, L.F. Cheng, C/C-SiC-ZrC composites fabricated by reactive melt infiltration with Si0.87Zr0.13 alloy, Ceram. Int. 38 (2012) 4337-4343

[17] D. Zhao, C.R. Zhang, H.F. Hu, Y.D. Zhang, Ablation behavior and mechanism of 3D C/ZrC composite in oxyacetylene torch environment, Compos. Sci. Technol. 71 (11) (2008) 1392-1396.

[18] Z.Y. Yan, Z. Ma, L. Liu, S.Z. Zhu, L.H. Gao, The ablation behavior of ZrB_2/Cu composite irradiated by high-intensity continuous laser, J. Eur. Ceram. Soc.

34(10)(2014)2203-2210.

[19] G.D Li, X. Xiong, K.L. Huang, Ablation mechanism of TaC coating fabricated by chemical vapor deposition on carbon-carbon composites, Trans. Nonferrous Met. Soc. China. 19(2009) 689-695.

[20] Q.M. Liu, L.T. Zhang, F.R. Jiang, J. Liu, L.F. Cheng, H. Li et al. Laser ablation behaviors of SiC-ZrC coated carbon/carbon composites, Surf. Coat. Technol. 205(17-18) (2011) 4299-4303.

[21] J.F. Ready, Effects due to absorption of laser radiation, J. Appl. Phys. 36 (1965) 462-470.

[22] H.O. Pierson, Handbook of Refractory Carbides and Nitride. Noyes Publications, New Jersey, 1996.P:68

[23] D.L. Schmidt, Ablative polymers in aerospace technology, in: G.F. D'Alelio, J.A.Parker (Eds.), Ablative Plastics, Marcel Dekker, New York, 1971, pp. 1-39.

[24] Y.G. Tong, S.X. Bai, H. Zhang, Y.C. Ye, Laser ablation behavior and mechanism of C/SiC composite, Ceram. Int. 39(6)(2013)6813-6820.

[25] D. Fang, Z.F. Chen, Y.D. Song, Z.G. Sun, Morphology and microstructure of 2.5 dimension C/SiC composites ablated by oxyacetylene torch, Ceram. Int. 35(2009)1249-1253.

[26] B.N. Chichkov, C. Momma, S. Nolte, A. Alvensleben, A. Tunnermann, Femtosecond, picosecond and nanosecond laser ablation of solids, Appl. Phys. A 63(1996)109-115.

Figure captions:

Fig.1 XRD patterns of the Si-Zr ARMI-C/C-SiC composite.

Fig.2 Typical cross-section microstructure of the Si-Zr ARMI-C/C-SiC composite (a) × 100 (b) ×1000.

Fig.3 Linear ablation rates of the Si-Zr ARMI-C/C-SiC composite and PIP-C/SiC composite versus the laser power densities.

Fig.4 Linear ablation rates of the Si-Zr ARMI-C/C-SiC composite and PIP-C/SiC composite versus the ablation time.

Fig.5 Surface morphologies of the Si-Zr ARMI-C/C-SiC composite ablated at 1000 W/cm^2 for 10s (a) and (b) three ablated regions on the ablated surface; (c) macro morphologies of the ablation center; (d) some small droplet on the ablated carbon fibers and pyrolytic carbon; (e) large magnification morphologies of the ZrC layer; (f) large magnification morphologies of the particles in transition zone; (g) ZrO_2 particles in some partial areas of transition zone.

Fig.6 Surface morphologies of the PIP-C/SiC composite ablated at 1000 W/cm^2 for 10s (a) the ablated deep pit on the ablated surface; (b) large magnification morphologies of the ablation center.

Fig.7 Surface morphologies of the Si-Zr ARMI-C/C-SiC composite ablated at 1000W/cm^2 for 30s (a) and (b) three ablated regions on the ablated surface; (c) macro morphologies of the ablation center; (d) large magnification morphologies of the ZrC layer.

Fig.8 Changes in Gibbs free energy as a function of temperature.

Fig.9 Laser ablation model for the Si-Zr ARMI-C/C-SiC composite (a) first stage dominated by the oxidation process; (b) second stage dominated by evaporation, decomposition and sublimation process; (c) third stage synergistically controlled by the scouring away of ZrC melt and evaporation, decomposition and sublimation process.